ELSEVIER

Surface Science 325 (1995) L385–L391

surface science

Surface Science Letters

Adsorbate structure and substrate relaxation for the Sb/Si(001)-(2 × 1) surface

P.F. Lyman [a], Y. Qian [a,b], M.J. Bedzyk [a,b]

[a] *Department of Materials Science and Engineering and Materials Research Center, Northwestern University, Evanston, IL 60208, USA*
[b] *Materials Science Division, Argonne National Laboratory, Argonne, IL 60439, USA*

Received 28 August 1994; accepted for publication 16 December 1994

Abstract

X-ray standing wave measurements were undertaken to study the bonding position of Sb adatoms on the Sb-saturated Si(001)-(2 × 1) surface. Using the (004) and (022) Bragg reflections, we find that the Sb atoms form dimers, and that the center of the Sb ad-dimers lies 1.64 Å above the bulk-like Si(004) surface atomic plane. When combined with a previous determination of the Sb–Si and Sb–Sb bond lengths, our results show that the surface Si plane is contracted inward by 0.10 Å upon saturation with Sb. Our in-plane results are compared to two structural models consisting of dimers whose bonds are parallel to the surface plane and whose centers are either shifted or unshifted (parallel to the dimer bond direction) relative to the underlying substrate planes. We thus find two special cases consistent with our data: one with symmetric (unshifted) dimers having a dimer bond length of 2.81 Å, and the other with midpoint-shifted dimers, having a bond length of 2.88 Å and a lateral shift of 0.21 Å.

1. Introduction

The structure and substrate response of the Sb-terminated Si(001) surface have implications for two technologically important phenomena in molecular beam epitaxy (MBE), namely surfactant-mediated epitaxy (SME) and construction of delta-doping layers. Ironically, SME relies on a near-total segregation of surface Sb atoms during growth, while delta-doping requires high incorporation rates. Clearly, understanding of the behavior and geometric structure of the Sb/Si surface is needed to learn under what conditions these nearly contrary requirements may be satisfied. Previous experimental investigations have brought low energy [1–4] and high energy [5,6] electron diffraction, core level spectroscopy [5,6], scanning tunneling microscopy (STM) [1,2,6], surface extended X-ray absorption fine structure (SEXAFS) [1], medium energy ion scattering [3] and transmission MeV ion channeling [4] to bear on various aspects of the problem. In addition, the stable bonding site and structure have been calculated using a first principles molecular cluster approach [7], and recently using a total energy slab calculation [8]. The picture that has arisen out of these investigations is one where Sb adsorption saturates at nearly one monolayer coverage (1 ML = 6.78×10^{14} cm^{-2}) at substrate temperatures above about 350°C. Locally, the well-known clean surface

* Corresponding author. Fax: +1 708 491 7820; E-mail: bedzyk@nwu.edu.

SSDI 0039-6028(94)00812-4

Si dimer reconstruction is lifted, and the adsorbed Sb atoms form new dimers on top of nearly bulk-like Si, similar to the behavior of As atoms on Si(001) [9]. The dimers are arranged in rows, resulting in the familiar (2×1) symmetry. As the pentavalent Sb atoms can form three bonds (and one lone-pair orbital), and the tetravalent, top-layer Si atoms can form four bonds, there are no dangling bonds, and the surface is rather passive [10]. The compressive strain induced by the mismatch in lattice size between Sb and Si, however, appears to cause numerous vacancy and antiphase defects in the Sb overlayer [2]. Thus, the saturation coverage of Sb is somewhat less than a full monolayer, ranging from 0.7 to 0.9 ML, depending on sample temperature and incident Sb species (Sb_4 or Sb_1) [3]. The breakup of the rows of dimers by defects and the high density of anti-phase boundaries imply a short coherence length for the domains of dimerized Sb. This explains the diffuseness and weakness of the half-order spots observed with electron diffraction [1–5]. One specific issue that has not yet been resolved is whether the Sb ad-dimer is symmetric, or if it is either tilted (as on clean Si(001) [11]) or shifted with respect to the underlying substrate (as on Sb/Ge(001) [12]).

In this Letter, we present an X-ray standing wave (XSW) investigation of the Sb-saturated Si(001) surface, employing reflections from the (004) and (022) bulk lattice planes. We thereby precisely determine several important Fourier components of the spatial distribution of Sb atoms relative to the Si lattice. We interpret these spatial distribution data in terms of several principal structural models of the Sb/Si(001) surface, and we thereby make (model-dependent) determinations of the Sb–Sb dimer bond length, asymmetric tilt, and midpoint shift. By combining our results with those of a previous SEXAFS experiment [1], which precisely measured the Sb–Si and Sb–Sb bond lengths, we can also determine the relaxation of the top Si layer. Our results thereby provide a stringent basis for comparison with ab initio calculations of the structure of this system.

2. Experimental procedure and results

The experiments were conducted at beamline X15A of the National Synchrotron Light Source at Brookhaven National Laboratory. The apparatus consists of several coupled ultrahigh vacuum (UHV) chambers (base pressure $\sim 9 \times 10^{-11}$ Torr) allowing sample preparation (MBE growth) and characterization (LEED, Auger electron spectroscopy (AES) and XSW). The XSW technique as well as the experimental arrangement at X15A have recently been extensively reviewed by Zegenhagen [13].

The Si(001) sample was Syton-polished and chemically cleaned ex situ using the Shiraki process [14], and then mounted in a strain-free manner. After degassing the sample in UHV, the Shiraki oxide was thermally desorbed at 900°C. The sample was then cooled to room temperature (initial cooling rate ~ 2.0°C/s), resulting in a sharp, two-domain (2×1) LEED pattern. AES could detect no O and a small amount of C contamination (~ 0.03 ML). With the Si substrate held at 550°C, ~ 3 ML of Sb was deposited from an effusion cell over 10 min. Since the sticking coefficient for Sb adsorption goes to zero at coverages near 1 ML [3], approximately 1 ML Sb was adsorbed on the surface. The Sb-saturated surface was further annealed for 5 min at 550°C, resulting in a (2×1) LEED pattern with slightly diffused half-order spots.

The incident X-ray beam from the synchrotron radiation source was collimated and monochromated by a double-crystal monochromator and directed through a Be window into the UHV chamber. The single crystal sample was held at room temperature and placed so that the X-ray beam was Bragg-reflected by either the (004) or the (022) set of diffraction planes. We used 6.23 keV X-rays for the (004) measurement, and 6.77 keV X-rays for the (022) measurement, and the resultant Sb L fluorescence yield was detected by a solid-state Si(Li) detector. The intensity of the Bragg-reflected X-ray beam was measured by an in vacuo Si photodiode. In the standard fashion [13], a rocking curve about the Bragg condition was accomplished by scanning the incident X-ray energy (using angular piezoelectric drives on both monochromator crystals). This is equivalent to scanning the angle of the sample substrate about the Bragg angle, and the abscissas of the data are therefore expressed as angular deflections. At each (equivalent) angular step, the reflected X-ray intensity and fluorescence spectrum were recorded simultaneously.

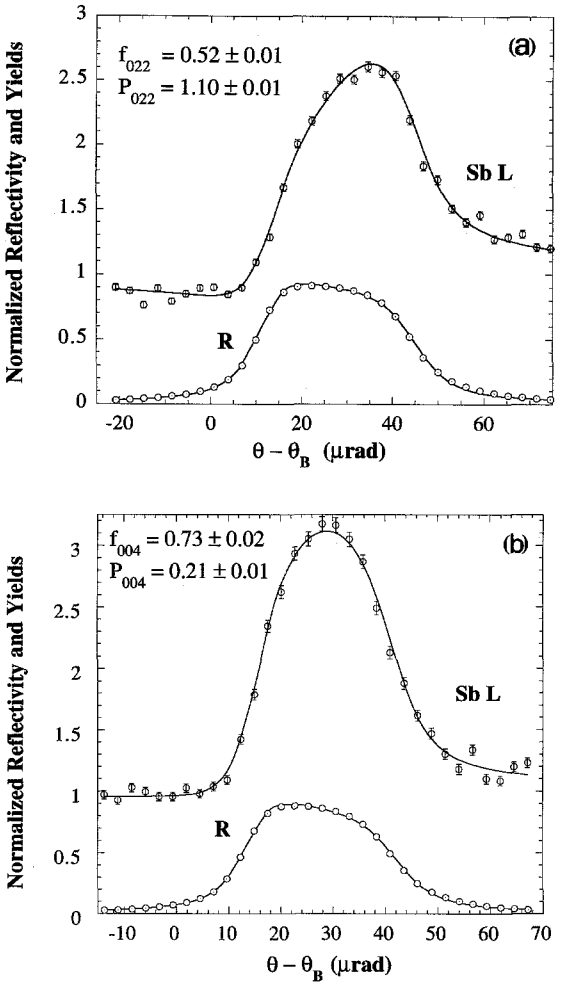

Fig. 1. The experimental and theoretical angular dependence for the X-ray reflectivity and Sb L fluorescence yield for: (a) the (004) reflection at $E_\gamma = 6.23$ keV, and (b) the (022) reflection at $E_\gamma = 6.77$ keV.

Fig. 1a shows the Si reflectivity and Sb L fluorescence yield (normalized to unity at off-Bragg angles) as a function of the Bragg reflection angle θ for the (004) reflection (diffraction vector normal to the sample surface). The solid line through the reflectivity data is a fit to standard dynamical diffraction theory [15]; the line through the fluorescence yield is a fit to a parametrization that will be discussed below. Fig. 1b shows similar data acquired for the same surface while scanning through the (022) reflection. Note that the (022) diffraction vector is tilted at 45° from the [004] surface normal direction, and that the two domains possible on this surface are equivalent with respect to this diffraction vector.

3. Discussion

The interference of the coherently coupled incident and Bragg-reflected X-ray plane waves generates an XSW in and above the crystal, with the XSW nodal planes parallel to and having the same periodicity as the diffraction planes. The phase of the standing wave with respect to the diffraction planes shifts by 180° as the Bragg angle θ is scanned from the low-angle side of the rocking curve to the high-angle side. This phase shift moves the antinodal planes of the standing wave inward by one-half of the d-spacing d_{hkl}. Thus, the angular dependence of the fluorescence yield $Y(\theta)$ from an adatom layer can be described as:

$$Y(\theta) = 1 + R(\theta) + 2\sqrt{R(\theta)}\, f_{c,H} \cos[v(\theta) - 2\pi P_H], \quad (1)$$

where $R(\theta)$ is the reflectivity and $v(\theta)$ is the relative phase of the diffracted plane wave. The coherent fraction $f_{c,H}$ and coherent position P_H correspond to the amplitude and phase, respectively, of the Hth Fourier component of the time-averaged spatial distribution of the nuclei of the adatoms (projected into a unit cell). $\boldsymbol{H}$ is the reciprocal lattice vector for the (hkl) diffraction planes. More specifically, the coherent fraction can be written as the product of three factors [16]:

$$f_{c,H} = C a_H D_H, \quad (2)$$

where C is the fraction of adatoms at ordered positions, a_H is a geometrical factor, and D_H is the Debye–Waller factor. The Debye–Waller factor can be written as $D_H = \exp[-2\pi^2 \langle u_H^2 \rangle / d_H^2]$, where $\langle u_H^2 \rangle$ is the mean-squared thermal vibrational amplitude of the adatom in the $\boldsymbol{H}$ direction.

While the information provided by an XSW scan, viz., the coherent fraction and coherent position, is unambiguous and completely model-independent, the process of determining structural parameters from these data is, however, somewhat model-dependent. Each XSW scan measures the amplitude and phase

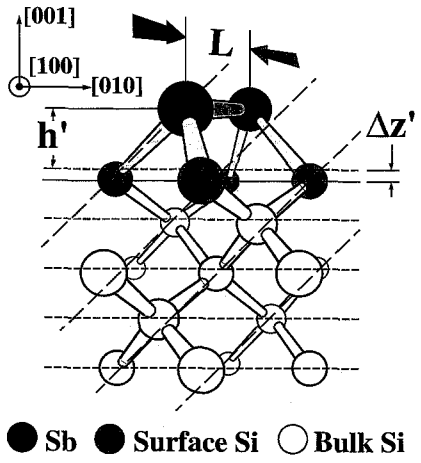

Fig. 2. A side view of the Sb/Si(001) surface ad-dimer model. The short dashed lines represent the Si(004) bulk-like lattice planes. The long dashed lines are the (022) bulk-like lattice planes. The solid line shows the height of the relaxed top Si layer. L is the Sb dimer bond length. (Note that the dimer bond does not lie in the plane of the figure.) h' is the height of the Sb dimer above the Si(004) bulk-like lattice planes. $\Delta z'$ is the inward relaxation of the top Si layer.

of a single Fourier component of the atomic spatial distribution; many such components are required to completely describe a complicated structure containing multiple inequivalent adatom sites. Without a complete set of Fourier components, therefore, we must make simplifying assumptions and employ symmetry arguments to deduce the structure. We will chiefly consider symmetric dimers, and briefly mention other possible structures consistent with our findings.

For symmetric Sb dimers, there are two ordered positions equally occupied by Sb atoms (see Fig. 2). The coherent position P_{004} equals h'/d_{004}, where h' locates the height of the Sb ad-dimer relative to the Si(004) bulk-like atomic plane. Based on symmetry considerations, the value of P_{022} should equal $(1 + P_{004})/2$ for symmetric dimers. The (004) geometrical factor a_{004} is unity, while the (022) geometrical factor would be:

$$a_{022} = |\cos(\pi L/2d_{022})|, \qquad (3)$$

where L is the Sb–Sb dimer bond length. The ambiguity in the interpretation of the experimental observables of XSW discussed above is essentially contained in the geometrical factor; similar expressions for a_H can be derived for other structural models.

The coherent fractions ($f_{c,004}$, $f_{c,022}$) and coherent positions (P_{004}, P_{022}) shown in Fig. 1 are determined by χ^2 fits of Eq. (1) to the Sb L fluorescence data. The measured value of $P_{004} = 1.21 \pm 0.01$ indicates that the Sb ad-dimer height $h' = P_{004} d_{004} = 1.64 \pm 0.02$ Å above the Si(004) bulk-like atomic planes. The measured value of P_{022} is 1.10 ± 0.01; the fact that this value is equivalent to $(1 + P_{004})/2$ confirms that the Sb atom *distribution* is symmetrically centered about one of the two-fold symmetry sites of the surface.

3.1. Substrate relaxation

In a SEXAFS experiment, Richter et al. [1] measured the bond lengths for this surface system, finding a Sb–Si bond length of 2.63 ± 0.04 Å and a Sb–Sb bond length of 2.88 ± 0.03 Å. Assuming a symmetric dimer geometry, the SEXAFS values imply that the Sb ad-dimer resides 1.74 ± 0.05 Å above the surface Si plane. Our XSW measurements indicate that the center of the Sb ad-dimer is located 1.64 ± 0.02 Å above the Si(004) bulk-extrapolated lattice planes. Therefore, we can conclude that at room temperature the top layer Si atoms on the saturated Sb/Si(001)-(2 × 1) surface are relaxed inward by 0.10 ± 0.05 Å.

Transmission MeV ion channeling has also been applied to this surface system [4]. This technique bears many similarities to XSW [17], as well as some important differences. A principal advantage of XSW compared to transmission MeV ion channeling is its superior precision (0.02 Å for XSW [13] versus about 0.1 Å for ion channeling [18]). Grant et al. [4] made a determination of the position of the Sb dimer above the bulk-like surface planes using transmission MeV ion channeling, and inferred the value of the Si surface plane relaxation. They reported a Si surface relaxation of 0.09 ± 0.07 Å, which was based on a symmetric dimer geometry, an assumed Sb–Si bond length of 2.63 Å, a measured Sb–Sb dimer length of 2.8 ± 0.1 Å and a measured height of the Sb atoms above the bulk-like surface plane of 1.63 ± 0.07 Å [4]; note, however, that the cited uncertainty in the relaxation does not include any contribution from uncertainty in the assumed Sb–Si bond length. The

ion channeling results are consistent with our measurements within cited experimental error. However, our XSW measurements provide a much more precise and more direct determination of these structural parameters, and furthermore are based entirely on experimentally determined quantities.

Our results for the Si relaxation also compare favorably to theoretical calculations of Group V/Si(001) adsorption systems. In a first-principles cluster calculation, Tang et al. [7] calculated the inward relaxation of the top layer Si atoms on the 1 ML Sb/Si(001)-(2 × 1) surface to be 0.05 ± 0.05 Å. Our result is also consistent with the pseudopotential calculation [9] of the relaxation of the As-terminated Si(001) surface, which should exhibit a relaxation comparable to the present case.

3.2. Dimer geometry

To describe the geometry of symmetric Sb dimers, we need to specify the Sb–Sb bond length L in addition to the height of the dimer bond above the surface. By using a diffraction vector with a component in the surface plane, such as the (022), we can determine this quantity using Eqs. (2) and (3). One must also know or calculate, however, the ordered fraction C and the Debye–Waller factor (or the thermal vibrational amplitude $\sqrt{\langle u_H^2 \rangle}$) for the Sb adatoms. To determine these three remaining quantities, there are only two remaining independent equations (those for $f_{c,004}$ and $f_{c,022}$). We must therefore make some simplifying assumptions; we will start by considering the vibrational amplitude. The ion channeling study reported a thermal vibration amplitude of $\sqrt{\langle u_H^2 \rangle} = 0.25 \pm 0.1$ Å for the Sb atoms on this surface at room temperature [4]. However, our XSW measured value of $f_{c,004} = 0.73 \pm 0.02$ implies that the maximum possible value for $\sqrt{\langle u_{004}^2 \rangle}$ is 0.18 Å. For our calculations of the remaining structural parameters (only), we will assume the thermal vibrational amplitude of Sb on the Sb/Si(001)-(2 × 1) surface at room temperature to be isotropic and equal to 0.12 ± 0.02 Å. This value agrees with the theoretical prediction calculated for the clean Si(001)-(2 × 1) surface [19], and is close to the room-temperature value inferred indirectly using XSW for the case of As/Si(001)-(2 × 1) [20]. Using this $\sqrt{\langle u_H^2 \rangle}$ value, the Debye–Waller factors are $D_{004} = 0.86 \pm 0.04$ and $D_{022} = 093 \pm 0.02$. Eqs. (2) and (3) then lead directly to a value of the Sb–Sb bond length L of 2.81 ± 0.09 Å. Note that this value is significantly shorter than that measured by SEXAFS [1], but that the uncertainty in our measurement does include that value. Calculations of the Sb bond length predict somewhat larger values, namely 2.93 ± 0.05 Å [7] and 2.96 Å [8].

As discussed above, the extraction of structural parameters from XSW-determined Fourier components depends somewhat on the structural model (in absence of a complete set of Fourier components). We will therefore briefly mention the implications of our data for other possible, but more complicated, structural models. Specifically, the Sb–Sb dimers might be tilted [11] and/or shifted [12] with respect to the underlying substrate. To determine structural parameters in the face of these additional degrees of freedom, we need to invoke additional constraints. While considering these more complicated structures, we assumed that the Sb–Sb bond length L = 2.88 ± 0.03 determined by SEXAFS [1] was correct. For this value of L, however, there is no non-zero tilt angle that is consistent with our data (with or without an accompanying midpoint shift). The ion-channeling data were also found to be inconsistent with tilted dimers [4], and so we will not consider further this class of structural models.

It is possible that the dimers remain parallel to the surface, but shifted along the bond direction, as was found for Sb/Ge(001) [12]. The (022) geometrical factor a_{022} is then a function of the bond length and the shift. Without additional in-plane Fourier components, we cannot uniquely determine the correct values of these parameters. However, we can specify a family of solutions. One special case is just that reported above, with zero shift and a bond length L of 2.81 ± 0.09 Å. If, however, we assume the SEXAFS value of L (2.88 Å) to be correct, then our results imply that the dimers must have a midpoint shift of 0.21 ± 0.10 Å. This interesting structure has never before been reported for a Group V/Si(001)-(2 × 1) surface system; for comparison, the shift in the Sb/Ge(001) system was found to be 0.16 Å [12].

Although it is not possible for us to conclude on the basis of the present data alone which of the allowed points in the family of shifted solutions is correct, we favor the symmetric-dimers model (i.e.,

Table 1
Theoretical and experimental values of structural dimensions for the 1 ML Sb/Si(001)-(2 × 1) surface

	Theory		Experiment		
	Dmol [a]	Slab (LDA) [b]	Ion channeling [c]	SEXAFS [d]	XSW [e]
L (Å)	2.93 ± 0.05 [f]	2.96	2.8 ± 0.1	2.88 ± 0.03	2.81 ± 0.09
h (Å)	1.73	1.70		1.74 ± 0.05	
h' (Å)			1.63 ± 0.07 [g]		1.64 + 0.02
$\Delta z' = h - h'$ (Å)	0.05 ± 0.05 [f]		0.09 ± 0.07 [h]	0.10 ± 0.05	

L is the Sb ad-dimer bond length. h and h' are the height of the Sb ad-dimer relative to the Si(001) surface atomic plane and the Si(004) bulk-like atomic planes, respectively. $\Delta z'$ represents the inward relaxation of the top layer Si(001) atoms.
[a] Ref. [7].
[b] Ref. [8].
[c] Ref. [4].
[d] Ref. [1].
[e] Present work; symmetric dimers assumed.
[f] Ref. [7] and private communication.
[g] Ref. [4] and private communication.
[h] Cited error bar assumes absolute certainty in Sb–Si bond length.

no shift), based on its simplicity and on chemical reasoning. Thus, we compare the structural parameters derived in this study under the assumption of symmetric dimers with previous theoretical and experimental studies of this surface system (Table 1). Our value for the bond length L barely agrees within experimental uncertainty with the value measured by SEXAFS (2.88 ± 0.03 Å) [1] or predicted by theoretical calculation (2.93 Å ± 0.05 Å) [7]. Our value is, however, in good agreement with that determined by ion channeling (2.8 ± 0.1 Å) [4]. In our study, the principal contribution to the relatively large uncertainty (0.09 Å) in the dimer bond length comes from our uncertainty in assuming a value for the Sb thermal vibrational amplitude. In the future, we will use higher-order harmonic XSW measurements [16] on this surface to determine additional Fourier components of the atomic distribution. With those data, we expect to be able to determine which of the structural models consistent with the present data is the correct one. Also, we can thus directly and more precisely measure the thermal vibration amplitudes $\sqrt{\langle u_{004}^2 \rangle}$ and $\sqrt{\langle u_{022}^2 \rangle}$, and hence reduce uncertainties in our Sb–Sb bond length measurements.

4. Conclusions

We have measured the position of Sb atoms on the saturated Sb/Si(001)-(2 × 1) surface using the XSW technique. We find that Sb atoms occur as dimers whose centers are located 1.64 ± 0.02 Å above the bulk-like Si lattice plane. Combined with previous SEXAFS measurements of the Sb–Si and Sb–Sb bond lengths, this implies an inward relaxation of the surface Si plane by 0.10 ± 0.05 Å. Our data are consistent with the class of structures having dimers whose midpoints may be shifted or unshifted parallel to the dimer bond direction. Tilted (or buckled) dimers are inconsistent with our findings. This work either demonstrates a structure never before reported for any Group V/Si(001)-(2 × 1) surface (shifted dimers), or it indicates that the Sb–Sb dimer bond length is significantly shorter than previously reported. Our measurements will be important in establishing a structural baseline for our upcoming experiments using Sb during SME, as well as for a stringent test of predictive theoretical calculations.

Acknowledgments

This work was supported by the US Department of Energy under contract No. W-31-109-ENG-38 to Argonne National Laboratory, contract No. DE-AC02-76CH00016 to National Synchrotron Light Source at Brookhaven National Laboratory, and by the National Science Foundation under contract No. DMR-9120521 to the MRC at Northwestern University. P.F.L. is partially supported by National Institutes of Health under award No. IR01KD45295-01.

References

[1] M. Richter, J.C. Woicik, J. Nogami, P. Pianetta, K.E. Miyano, A.A. Baski, T. Kendelewicz, C.E. Bouldin, W.E. Spicer, C.F. Quate and I. Lindau, Phys. Rev. Lett. 65 (1990) 3417.
[2] J. Nogami, A.A. Baski and C.F. Quate, Appl. Phys. Lett. 58 (1991) 475.
[3] W.F.J. Slijkerman, P.M. Zagwijn, J.F. van der Veen, D.J. Gravesteijn and G.F.A. van de Walle, Surf. Sci. 262 (1992) 25.
[4] M.W. Grant, P.F. Lyman, J.H. Hoogenraad and L.E. Seiberling, Surf. Sci. 279 (1992) L180; private communication.
[5] D.H. Rich, T. Miller, G.E. Franklin and T.-C. Chiang, Phys. Rev. B 39 (1989) 1438.
[6] D.H. Rich, F.M. Leibsle, A. Samsavar, E.S. Hirschorn, T. Miller and T.-C. Chiang, Phys. Rev. B 39 (1989) 12758.
[7] S. Tang and A.J. Freeman, Phys. Rev. B 47 (1993) 1460; B 48 (1993) 8068; private communnication.
[8] B.D. Yu and A. Oshiyama, Phys. Rev. B 50 (1994) 8942.
[9] R.I. Urhberg, R.D. Bringans, R.Z. Bachrach and J.E. Northrup, Phys. Rev. Lett. 56 (1986) 520.
[10] R.D. Bringans, D.K. Biegelsen, J.E. Northrup and L.-E. Swartz, Jpn. J. Appl. Phys. 32 (1993) 1484.
[11] R.A. Wolkow, Phys. Rev. Lett. 68 (1992) 2636, and references therein.
[12] M. Lohmeier, H.A. van der Vegt, R.G. van Silfhout, E. Vlieg, J.M.C. Thornton, J.E. Macdonald and P.M.L.O. Scholte, Surf. Sci. 275 (1992) 190.
[13] J. Zegenhagen, Surf. Sci. Rep. 18 (1993) 199.
[14] A. Ishizaka and Y. Shiraki, J. Electrochem. Soc. 133 (1986) 666.
[15] B.W. Batterman and H. Cole, Rev. Mod. Phys. 36 (1964) 681.
[16] M.J. Bedzyk and G. Materlik, Phys. Rev. B 31 (1985) 4110.
[17] J.A. Golovchenko, B.W. Batterman and W.L. Brown, Phys. Rev. B 10 (1974) 4239.
[18] L.C. Feldman, J.W. Mayer and S.T. Picraux, Materials Analysis by Ion Channeling (Academic Press, New York, NY, 1982).
[19] O.L. Alerhand, J.D. Joannopoulos and E.J. Mele, Phys. Rev. B 39 (1989) 12622.
[20] G.E. Franklin, E. Fontes, Y. Qian, M.J. Bedzyk, J.A. Golovchenko and J.R. Patel, Phys. Rev. B 50 (1994) 7483.